

# The inability of vaccinia virus A33R protein to form intermolecular disulfide-bonded homodimers does not affect the production of infectious extracellular virus

Winnie M. Chan, Aja E. Kalkanoglu<sup>1</sup>, Brian M. Ward<sup>\*</sup>

Department of Microbiology and Immunology, University of Rochester Medical Center, Rochester, New York 14642, USA

## ARTICLE INFO

### Article history:

Received 23 August 2010  
 Returned to author for revision  
 10 September 2010  
 Accepted 19 September 2010  
 Available online 13 October 2010

### Keywords:

Vaccinia virus  
 A33R  
 Morphogenesis  
 Intermolecular disulfide bond

## ABSTRACT

The orthopoxvirus protein A33 forms a disulfide-bonded high molecular weight species that could be either a homodimer or a heteromultimer. The protein is a major target for neutralizing antibodies and the majority of antibodies raised against A33 only recognize the disulfide-bonded form. Here, we report that A33 is present as a disulfide-bonded homodimer during infection. Additionally, we examined the function of intermolecular disulfide bonding in A33 homodimerization during infection. We show that the cysteine at amino acid 62 is required for intermolecular disulfide bonding, but not dimerization as this mutant was still able to form homodimers. To investigate the role of disulfide-bonded homodimers during viral morphogenesis, recombinant viruses that express an A33R with cysteine 62 mutated to serine were generated. The recombinant viruses had growth characteristics similar to their parental viruses, indicating that intermolecular disulfide-bonded homodimerization of A33 is not required for its function.

© 2010 Elsevier Inc. All rights reserved.

## Introduction

Vaccinia virus, which was used as a live-attenuated vaccine to eradicate smallpox, belongs to the Poxviridae family. It has a large double-stranded DNA genome of 200 kb, and the genome is predicted to encode approximately 200 functional open reading frames (Moss, 2001). Unlike most DNA viruses, poxviruses replicate entirely in the cytoplasm of infected cells in a specialized area known as the viral factory. The first form of infectious virions produced from the viral factory is called intracellular mature virions (IMV). IMV represent the majority of virions produced from an infected cell and remain within the infected cell. A subset of IMV obtain an additional double membrane envelope as the result of wrapping that occurs at the *trans*-Golgi network (TGN) or early endosome to become intracellular enveloped virions (IEV) (Hiller and Weber, 1985; Schmelz et al., 1994; Tooze et al., 1993). IEV are transported from the site of wrapping to the cell surface along microtubules and are released from the cytoplasm by fusion of their outermost membrane with the plasma membrane (Geada et al., 2001; Hollinshead et al., 2001; Rietdorf et al., 2001; Ward and Moss, 2001a). Released virions retained on the cell surface are called cell-associated enveloped virions (CEV). CEV are required for the induction of actin tails and, hence, efficient cell-to-cell spread (Smith et al., 2002; Ward and Moss, 2001a). A subset of CEV

are released from the cell surface and become extracellular enveloped virions (EEV), which are responsible for long-range dissemination of virus (Appleyard et al., 1971; Payne, 1980). Collectively, CEV and EEV make up what are termed extracellular virions (EV).

Seven virus-encoded proteins, A33, A34, A36, A56, B5, F12, and F13, have been shown to be specific for the enveloped forms, IEV, CEV, and EEV, (Duncan and Smith, 1992; Engelstad et al., 1992; Isaacs et al., 1992; Roper et al., 1996; van Eijl et al., 2002, 2000). Of these seven proteins, A36 and F12 are exclusive to IEV (van Eijl et al., 2002, 2000; Wolffe et al., 2001). A36 is involved in virion transport along microtubules, while F12 is involved in virion egress (van Eijl et al., 2002; Ward et al., 2003). The complex of A56 and K2 is known as fusion regulatory proteins and associates with the entry/fusion complex (Wagenaar and Moss, 2007). B5 and F13 have been shown to be required for morphogenesis as deletion of either one of these genes results in a decrease in enveloped virion production (Blasco and Moss, 1991; Isaacs et al., 1992). Deletion of either A33 or A34 increases the amounts of EEV released into the media, and therefore, they are believed to be involved in retention of CEV (Chan and Ward, 2010; McIntosh and Smith, 1996; Roper et al., 1998).

A33 is a type II integral membrane protein that forms disulfide-bonded homodimers or heteromultimers (Roper et al., 1996). It coordinates the incorporation of A36 into IEV membranes and, subsequently, the production of actin tails (Wolffe, Weisberg, and Moss, 2001). Deletion of A33R causes a small plaque phenotype. This phenotype is due to a number of defects, including the inability to form actin tails and a reduction in the infectiousness of EV (Chan and Ward, 2010; Roper et al., 1998). A33 is a major target for antibody neutralization of the enveloped form of the virus and is a potential

<sup>\*</sup> Corresponding author. Department of Microbiology and Immunology, University of Rochester, 601 Elmwood Avenue, Box 672, Rochester, NY 14642. Fax: +1 585 473 9573.

E-mail address: [Brian\\_Ward@urmc.rochester.edu](mailto:Brian_Ward@urmc.rochester.edu) (B.M. Ward).

<sup>1</sup> Current address: Pulmonary and Critical Care Department, University of Rochester, Rochester, NY 14642.

candidate for a subunit vaccine against orthopoxvirus infections (Hooper et al., 2003, 2004). Either passive transfer of A33 monoclonal antibodies or vaccination with an A33R subunit vaccine, delivered as either DNA or recombinant protein, confers protection against a lethal poxvirus challenge in animal models (Fang et al., 2006; Fogg et al., 2004; Hooper et al., 2000). A33 contains six cysteine residues: one in the predicted cytoplasmic tail and five in the predicted extracellular domain. We wanted to examine if intermolecular disulfide bonding of A33 was required for its function during infection and, therefore, mapped the cysteine(s) involved in intermolecular disulfide bonding. While we were carrying out these experiments, a partial structure of A33 was determined (Su et al., 2010). Although the partial structure did not contain the cysteine at position 62 (C62), the authors predicted that C62 was involved in intermolecular disulfide bonding (Su et al., 2010). Here, we show that C62 is indeed required for intermolecular disulfide-bonded homodimerization of A33 and that A33 lacking the cysteine at amino acid 62 still forms homodimers. In addition, we examined the function of intermolecular disulfide bonding of A33 utilizing recombinant viruses that express A33R containing cysteine-to-serine mutation at amino acid 62. Characterization of the recombinants revealed that disulfide-bonded homodimerization of A33 is not required for the production of infectious extracellular virions.

## Results

### Cysteine at amino acid position 62 is involved in intermolecular disulfide bond formation

While A33 is predicted to encode a 21-kDa protein, it was shown to migrate at 55 kDa under non-reducing conditions and a smear at 23–28 kDa under reducing conditions, indicating that it forms either a homodimer or a heteromultimer that is disulfide-bonded (Roper et al., 1996). There are six cysteine residues in A33: one in the predicted

cytoplasmic tail and five in the predicted luminal domain (Fig. 1A). We wanted to map the cysteine(s) involved in intermolecular disulfide bond formation and, hence, homodimerization. Therefore, the six cysteines in A33 were individually mutated to the structurally similar amino acid, serine, and analyzed by Western blot under either reducing or non-reducing conditions. As shown in Fig. 1B, the A33-HA<sup>C62S</sup> mutant was detected as a band that is consistent with a monomer under both reducing and non-reducing conditions. In contrast, the other mutants, A33-HA<sup>C36S</sup>, A33-HA<sup>C100S</sup>, A33-HA<sup>C109S</sup>, A33-HA<sup>C126S</sup>, and A33-HA<sup>C180S</sup>, along with A33-HA, were only detected as monomers under reducing conditions and as forms consistent with dimers and tetramers under non-reducing conditions (Fig. 1B). Our results demonstrated that C62 is required for intermolecular disulfide-bonded homodimerization. Several monoclonal antibodies raised against A33 are conformation-specific and are only able to detect unreduced A33 (Chen et al., 2007; Golden and Hooper, 2008). This raises the possibility that the epitope recognized by those monoclonal antibodies spans the two subunits of an A33 homodimer. To test this possibility, we determined if the A33-HA<sup>C62S</sup> mutant could be recognized by the conformation-specific antibody, MAb-10F10 (Golden and Hooper, 2008). As expected, MAb-10F10 recognized forms consistent with dimers and tetramers in unreduced lysates from cells expressing A33-HA and A33-HA<sup>C36S</sup> (Fig. 1B). It only recognized the monomeric form of the A33-HA<sup>C62S</sup>, indicating that the epitope is contained within a single monomer of A33. In contrast, it did not recognize the unreduced forms of A33-HA<sup>C100S</sup>, A33-HA<sup>C109S</sup>, A33-HA<sup>C126S</sup>, and A33-HA<sup>C180S</sup>.

### Intermolecular disulfide bonding of A33 is not required for interaction with B5-GFP

Interaction between A33 and B5, another enveloped-specific protein encoded by the virus, has been reported (Perdiguerro and Blasco, 2006). We have found that A33 interacts with B5-GFP in the

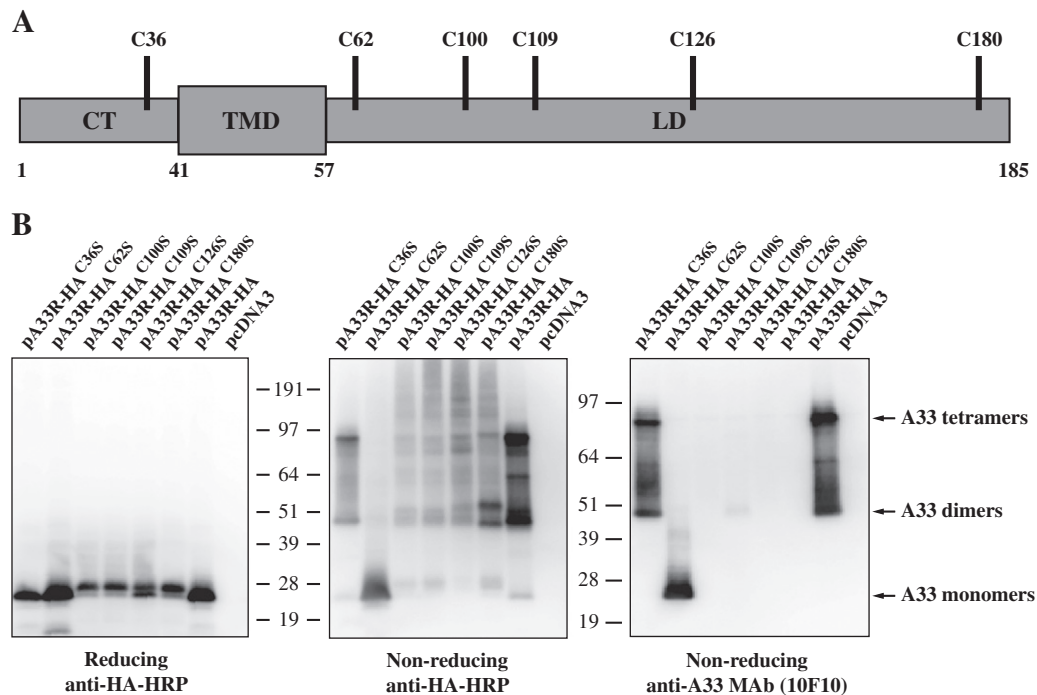


**Fig. 1.** Cysteine at amino acid 62 is involved in intermolecular disulfide bond formation. (A) Schematic representation of A33. A33 is a type II transmembrane protein. The predicted cytoplasmic tail (CT), transmembrane domain (TMD), and luminal domain (LD) are shown. The positions of the six cysteine residues are indicated. (B) Western blot analysis. HeLa cells were infected with vTF7.3 in the presence of AraC and transfected with the indicated plasmids. 24 h PI, cells were harvested and lysed. Cell lysates were resolved by SDS-PAGE under either reducing or non-reducing conditions. The proteins were transferred to nitrocellulose. The membranes were probed with an HRP-conjugated anti-HA antibody or anti-A33 MAb (10F10). The positions and molecular weights, in kilodalton, of marker proteins are shown.

absence of other viral late proteins and that A33 is required for B5-GFP to be efficiently incorporated into enveloped virions, suggesting that the interaction of A33 and B5-GFP may be necessary for B5-GFP incorporation (Chan and Ward, 2010) (Chan and Ward, unpublished). Therefore, we performed co-immunoprecipitation to determine if our A33 cysteine-to-serine mutants were still capable of interacting with B5-GFP. All of the A33 cysteine-to-serine mutants brought down a band of the predicted size for B5-GFP (Fig. 2), indicating that all of them are capable of interacting with B5-GFP. Furthermore, A33-HA, A33-HA<sup>C36S</sup>, and A33-HA<sup>C62S</sup> immunoprecipitated similar amount of B5-GFP. In contrast, A33-HA<sup>C100S</sup>, A33-HA<sup>C109S</sup>, A33-HA<sup>C126S</sup>, and A33-HA<sup>C180S</sup> immunoprecipitated more B5-GFP compared to A33-HA (Fig. 2). To rule out the possibility that the increased levels of B5-GFP co-immunoprecipitated with these mutants was not due to differences in B5-GFP expression levels, cell lysates were analyzed by Western blot using an anti-GFP antibody. As shown in Fig. 2, equivalent levels of B5-GFP were expressed, indicating that the greater amount of B5-GFP co-immunoprecipitated with these mutants was not due to higher expression levels of B5-GFP. The results were identical when B5 was used in place of B5-GFP (data not shown).

### A33<sup>C62S</sup> still forms homodimers

A recombinant A33 expressed in bacterial cells that does not contain amino acid residues 1 to 89 has been reported to exist as a stable homodimer (Su et al., 2010). We, therefore, wanted to

determine if full-length A33-HA<sup>C62S</sup> expressed in eukaryotic cells could still form homodimers in the absence of intermolecular disulfide bonding. To test this, we generated A33<sup>C62S</sup> with a V5-epitope tag on its cytoplasmic tail (pV5-A33R<sup>C62S</sup>) and examined if normal A33-HA or A33-HA cysteine-to-serine mutants could interact with V5-A33<sup>C62S</sup> using co-immunoprecipitation. All of the A33-HA cysteine-to-serine mutants, including A33-HA<sup>C62S</sup>, co-immunoprecipitated a band of the predicted size for V5-A33<sup>C62S</sup> (Fig. 3A), indicating that the full-length A33-HA<sup>C62S</sup> can still dimerize when expressed in eukaryotic cells. We also observed that A33-HA<sup>C100S</sup>, A33-HA<sup>C109S</sup>, A33-HA<sup>C126S</sup>, or A33-HA<sup>C180S</sup> brought down more V5-A33<sup>C62S</sup> than the unmutated A33-HA (Fig. 3A). To ensure that V5-A33<sup>C62S</sup> was expressed at similar levels, cell lysates were analyzed by Western blot using an anti-V5 antibody. As shown in Fig. 3C, the greater amount of V5-A33<sup>C62S</sup> brought down with these mutants was not due to a higher expression level of V5-A33<sup>C62S</sup>.

### Generation of A33R<sup>C62S</sup> recombinant viruses

Our data indicate that A33<sup>C62S</sup> was still capable of forming homodimers. We wanted to examine if A33<sup>C62S</sup> could replace A33 during infection even though it is incapable of forming disulfide-bonded dimers. Therefore, we generated recombinant viruses expressing A33R<sup>C62S</sup> that contains a serine at amino acid 62 in place of normal A33R and either B5R-GFP (vB5R-GFP/A33R<sup>C62S</sup>) or normal B5R (vA33R<sup>C62S</sup>). We generated recombinant viruses that express A33R<sup>C62S</sup> in both vB5R-GFP and WR backgrounds because we have previously shown that a recombinant virus that expresses B5R-GFP and has A33R deleted produces smaller plaques than a recombinant virus that only has A33R deleted, indicating that B5R-GFP is a more sensitive indicator of defects in A33 (Chan and Ward, 2010).

Our initial analysis of A33<sup>C62S</sup> was conducted in the absence of late viral protein synthesis. We wanted to determine if A33<sup>C62S</sup> could form disulfide-bonded homodimers during infection. Lysates of infected cells were analyzed under reducing and non-reducing conditions by Western blot using a polyclonal anti-A33 antibody. A33 has been shown to migrate between 23 and 28 kDa on SDS-PAGE under reducing conditions (Roper et al., 1996). As expected, A33<sup>C62S</sup> was detected as a monomer under both reducing and non-reducing conditions (Fig. 4). Normal A33 migrated at sizes consistent with monomers, dimers, and tetramers under non-reducing conditions but only as a monomer under reducing conditions (Fig. 4). To examine if the conformation of A33<sup>C62S</sup> is retained in the presence of other viral proteins, we performed Western blots using MAb-10F10 under either reducing or non-reducing conditions. Consistent with our previous results, MAb-10F10 only recognized the monomeric form of A33<sup>C62S</sup> and only under non-reducing conditions (Fig. 4).

### A33<sup>C62S</sup> localizes properly in infected cells

We next examined the intracellular localization of A33<sup>C62S</sup> in infected cells using immunofluorescence microscopy. In cells infected with WR or vB5R-GFP, A33 localized at the site of wrapping, at the cell vertices, and on virion-sized particles in the cytoplasm (Fig. 5). In cells infected with either vB5R-GFP/A33R<sup>C62S</sup> or vA33R<sup>C62S</sup>, the localization pattern of A33<sup>C62S</sup> was identical to that seen in cells infected with the parental viruses, WR and vB5R-GFP (Fig. 5). In addition, we also examined the localization of B5 or B5-GFP in infected cells. In cells infected with WR, vB5R-GFP, vB5R-GFP/A33R<sup>C62S</sup>, or vA33R<sup>C62S</sup>, B5-GFP or B5 localization appeared normal with all three of the characteristic hallmarks present, localization to the site of wrapping, the cell vertices, and on virion-sized particles (Fig. 5) (Ward and Moss, 2001b). As had been shown before, all three characteristic hallmarks of B5 localization were not observed in cells infected with either vΔA33R or vB5R-GFP/ΔA33R (Fig. 5) (Chan and Ward, 2010). The ability of A33<sup>C62S</sup> to restore proper localization of B5/B5-GFP in cells

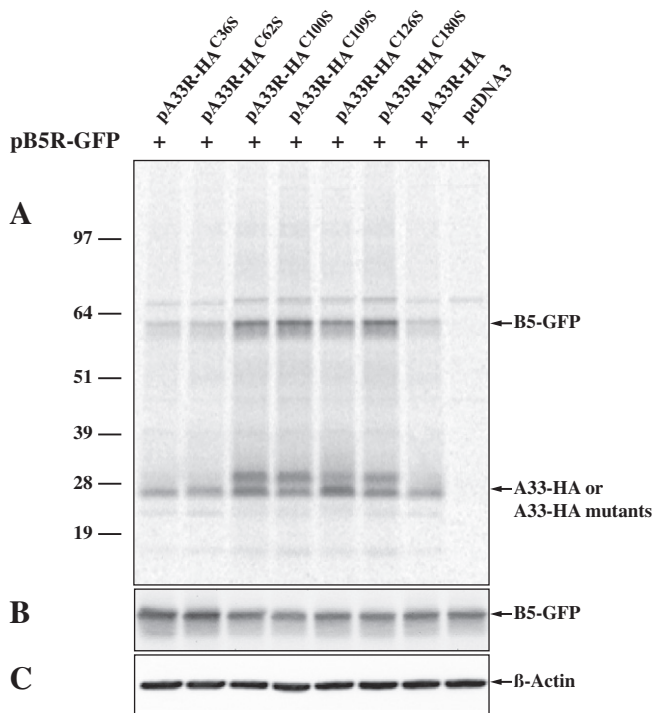


**Fig. 2.** A33-HA<sup>C62S</sup> interacts with B5-GFP. HeLa cells, infected with vTF7.3 in the presence of AraC and transfected with the indicated plasmids, were incubated with media containing [<sup>35</sup>S]-Met/Cys at 4 h post-transfection. 24 h PI, cells were harvested and lysed in RIPA buffer. Cell lysates were subjected to immunoprecipitation with an anti-HA MAb. Antibody-protein complexes (A) or cell lysates (B and C) were resolved by SDS-PAGE. Radiolabeled proteins were detected by autoradiography (A). The positions and molecular weights, in kilodalton, of marker proteins are shown. The levels of B5-GFP (B) and β-actin (C) in the cell lysates were detected by Western blot using an HRP-conjugated anti-GFP antibody or an anti-β-actin MAb, followed by an HRP-conjugated donkey anti-mouse antibody, respectively.

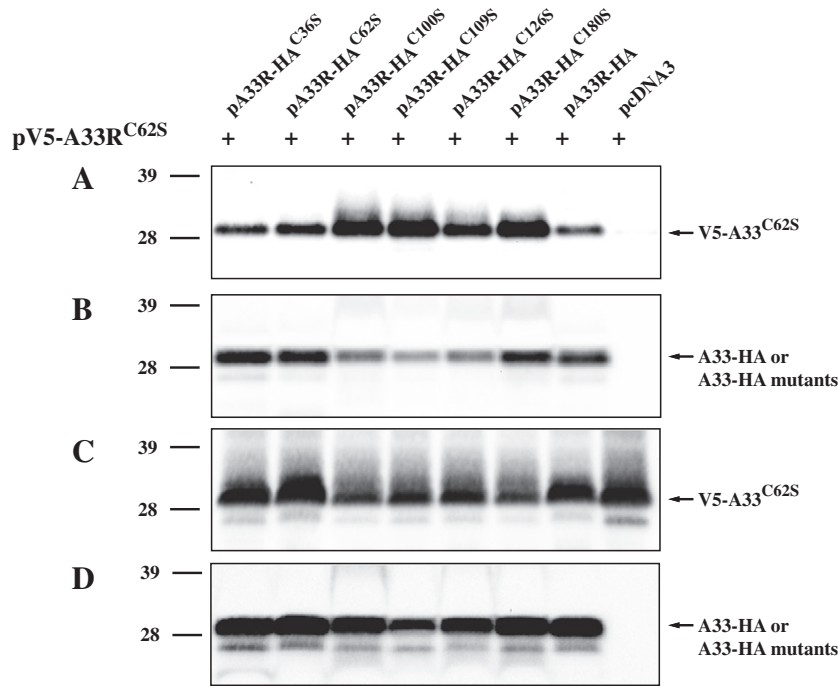


**Fig. 3.** A33-HA<sup>C62S</sup> forms dimers. HeLa cells were infected with vTF7.3 in the presence of AraC and transfected with the indicated plasmids. 24 h PI, cells were harvested and lysed in RIPA buffer. A33-HA or A33-HA cysteine-to-serine mutants were immunoprecipitated with an anti-HA Mab. Immune complexes (A and B) or cell lysates (C and D) were resolved by SDS-PAGE. V5-A33<sup>C62S</sup> was detected by Western blotting with an HRP-conjugated anti-V5 antibody (A and C). After probing with an anti-V5 antibody, the blots were stripped and re-probed with an HRP-conjugated anti-HA antibody (B and D). The positions and molecular weights, in kilodalton, of marker proteins are shown.

infected with a recombinant virus that has A33R deleted indicates that A33<sup>C62S</sup> appears to function normally during infection.

#### A33R<sup>C62S</sup> recombinant viruses form normal-sized plaques

Plaque size indicates the ability of orthopoxviruses to produce infectious enveloped virions and their ability to spread from cell to cell. To examine if infectious enveloped virions are produced by A33R<sup>C62S</sup> recombinants, we compared the plaques made by our recombinant viruses expressing A33R<sup>C62S</sup> to those made by the parental viruses. Both vB5R-GFP/A33R<sup>C62S</sup> and vA33R<sup>C62S</sup> produced plaques similar in size to those made by the parental viruses (Fig. 6), indicating that intermolecular disulfide bonding of A33 is not required for infectious enveloped virion production and actin tail formation. Taken together, vB5R-GFP/A33R<sup>C62S</sup> and vA33R<sup>C62S</sup> had similar subcellular localization (Fig. 5) and produced similar sized plaques on cell monolayer (Fig. 6), indicating that they are identical. Therefore, further characterization was only carried out on vA33R<sup>C62S</sup>.

#### The replication kinetics of vA33R<sup>C62S</sup> is similar to that of WR

Our previous result indicated that preventing the formation of intermolecular disulfide-bonded A33 homodimers did not cause a defect in infectious enveloped virion production (Fig. 6). To compare the replication kinetics of vA33R<sup>C62S</sup> to that of WR, we determined the amounts of infectious virions produced by WR or vA33R<sup>C62S</sup> using a low MOI growth curve, which directly looks at the production of infectious enveloped virions and their ability to spread from cell to cell. We determined the amounts of infectious virions released into the media and virions associated with the cells using plaque assays. The titers of infectious virions released from the cells and associated with the cells were identical between vA33R<sup>C62S</sup> and WR (Fig. 7), showing that disruption of the intermolecular disulfide bonding between A33 monomers does not have a noticeable effect on infectious virion production.

vA33R<sup>C62S</sup> and WR produce similar amounts of infectious EEV and CEV

Analysis of the growth property of vA33R<sup>C62S</sup> showed no detectable defect. A33 has been shown to be required for optimal production of fully infectious EEV and CEV (Chan and Ward, 2010). We next examined the infectivity of EEV and CEV produced by vA33R<sup>C62S</sup> and compared it to WR. The amounts of EEV and CEV produced by cells infected with either WR or vA33R<sup>C62S</sup> were determined using real-time PCR to quantify the genomes and plaque assays to determine their infectivity. We found that vA33R<sup>C62S</sup> produced similar amounts of EEV and CEV genome copies as well as infectious EEV and CEV compared to WR (Fig. 8). Taken together, the intermolecular disulfide bonding between A33 monomers appears not to be required for its functions.

#### Discussion

A33 is one of seven enveloped virus-specific proteins encoded by orthopoxviruses and is found in all of the members of the subfamily Chordopoxvirinae, except for the members of the *Avipoxvirus* genus (Roper et al., 1996). A33 was reported to be a disulfide-bonded multimer in infected cells and has been reported to be palmitoylated (Payne, 1992; Roper et al., 1998). The six cysteine residues in A33 are highly conserved among the members of the subfamily Chordopoxvirinae. Of these six cysteine residues, C36 is predicted to be palmitoylated as it is the only cysteine in the cytoplasmic tail (Grosenbach et al., 2000; Payne, 1992). Of the remaining five cysteines, C100, C109, C126, and C180 were recently reported to be involved in intramolecular disulfide bond formation (Su et al., 2010). Based on this finding, it was predicted that C62 would be involved in intermolecular disulfide bonding of A33. Here, we show that C62 is involved in linking two monomers covalently via a disulfide bond. Interestingly, we found that disruption of the ability to form the intermolecular disulfide bond did not prevent the formation of A33 homodimers. Subsequently, disruption of intermolecular disulfide



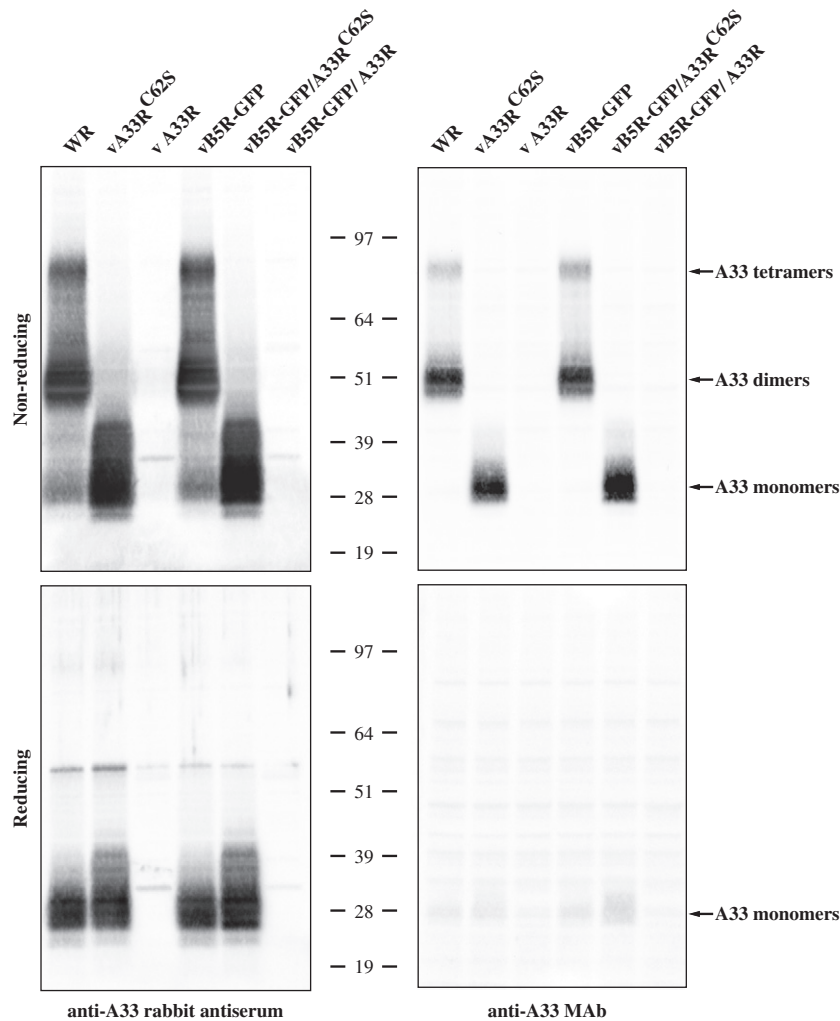


**Fig. 4.** A33<sup>C62S</sup> is detected as a monomer under both reducing and non-reducing conditions. HeLa cells were infected with the indicated viruses at a MOI of 10.0. 24 h PI, cells were harvested and lysed in RIPA buffer. Cell lysates were resolved by SDS-PAGE under either reducing or non-reducing conditions and Western blotted with either an anti-A33 rabbit antiserum or anti-A33 MAb. The positions and molecular weights, in kilodalton, of marker proteins are shown.

bond formation did not cause any detectable defect in A33 function during infection.

The fact that A33<sup>C62S</sup> still formed dimers establishes that there are two mechanisms for homodimerization, one is through the intermolecular disulfide bonding at C62 and the other, through interaction between the specific residues in the dimer interface. There have been two functions reported for A33 during viral infection. A33 has been reported to coordinate the inclusion of viral proteins into the IEV wrapping membrane (Wolffe et al., 2001). In addition, A33 contains a C-type lectin-like domain that has been postulated to bind EV to the cell surface (Su et al., 2010). It is unclear if A33 needs to be a dimer for complete functionality during infection. The redundant mechanisms for dimerization are indicative that it does. A recent report indicated that the structure of the A33 homodimer contained dimers of the C-type lectin-like domain, indicating that each monomer contains the domain, and therefore, should be capable of binding ligand (Su et al., 2010). It is unclear if A33 needs to be a dimer for it to coordinate protein incorporation into the IEV membrane. It would be interesting to identify the region of homodimerization in A33 in order to determine if A33 can function as a monomer during infection.

A study has shown that vaccination with vaccinia virus elicits long-lived antibody responses directed against virus-specific membrane proteins in humans, one of which is A33 (Lawrence et al., 2007). In addition, all of the vaccine recipients elicited anti-A33 antibodies after

vaccination, and therefore, A33 has been suggested for inclusion in a potential subunit vaccines against orthopoxviruses (Lawrence et al., 2007). The majority of monoclonal antibodies raised against A33 only recognize unreduced A33, and therefore, the dimeric form (Chen et al., 2007; Golden and Hooper, 2008; Roper et al., 1996). Surprisingly, A33<sup>C62S</sup> is recognized as a monomer by a conformation-specific anti-A33 monoclonal antibody under non-reducing conditions, indicating that the antibody recognition epitope does not span the two monomers (Figs. 1 and 4). Conversely, A33-HA<sup>C100S</sup>, A33-HA<sup>C109S</sup>, A33-HA<sup>C126S</sup>, and A33-HA<sup>C180S</sup> were not detected by the conformation-specific antibody (Fig. 1B). These cysteines were reported to be involved in intramolecular disulfide bonding and are required for conformation, which is apparently required for recognition by MAb-10F10 (Su et al., 2010). Several studies have used a recombinant A33 protein for vaccination studies to look at its ability to protect against a lethal orthopoxvirus infection (Buchman et al., 2010; Fang et al., 2006; Fogg et al., 2004). The A33 protein used in these studies still contained C62 and formed disulfide-bonded homodimers. Our results suggest that a monomer of A33 should be just as immunogenic.

A33 is detected as both a dimer and a tetramer under non-reducing conditions (Fig. 4), raising the possibility that an additional disulfide bond forms between two homodimers. Tetramer formation appears to require intermolecular disulfide bonded homodimers because mutating C62 abrogates A33 tetramer formation (Fig. 4).

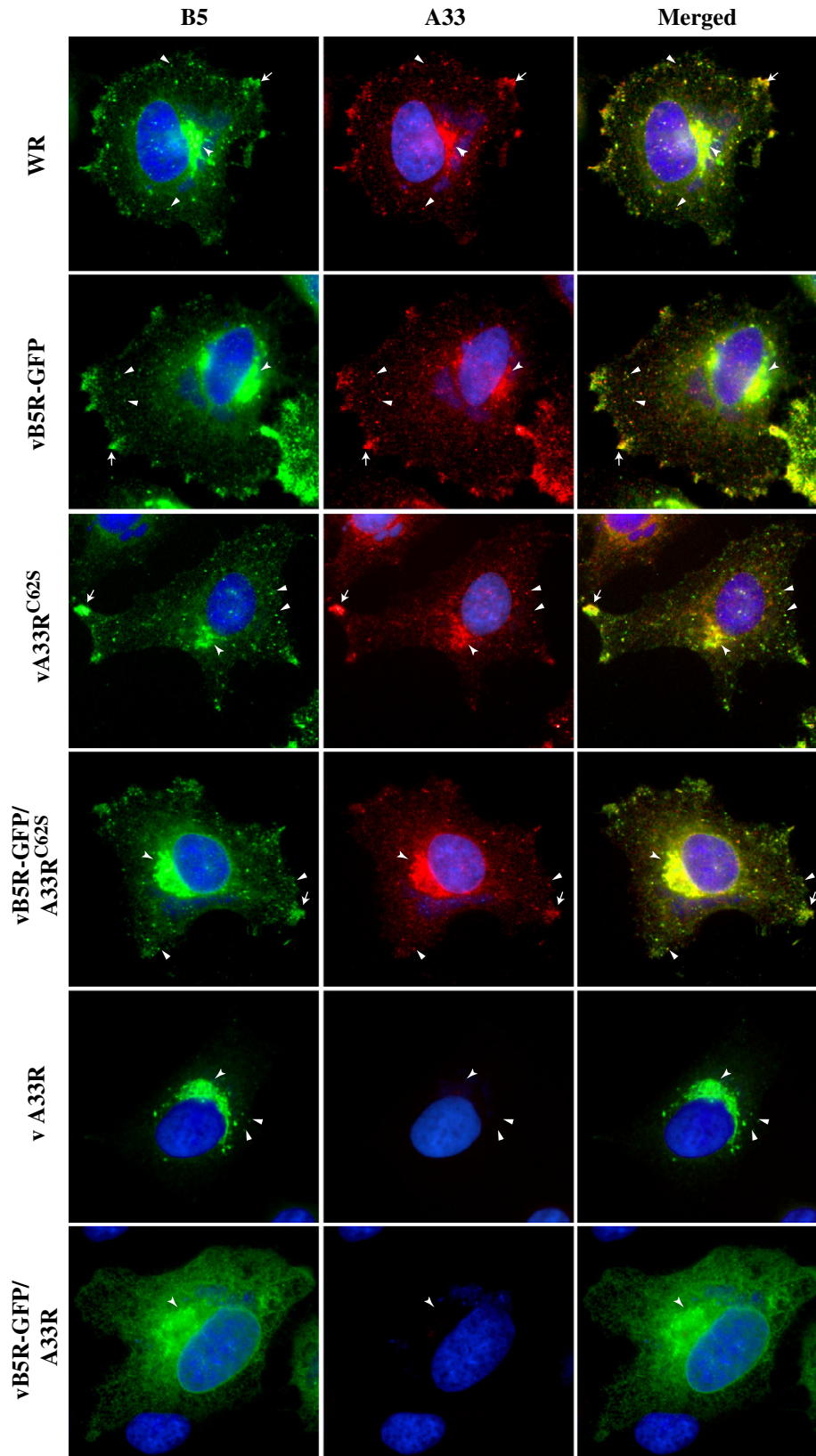


**Fig. 5.** Disulfide-bonded homodimerization is not required for proper localization of A33. HeLa cells grown on glass coverslips were infected with the indicated viruses at a MOI of 1.0. The next day, cells were fixed, permeabilized, and stained with an anti-A33 MAb, followed by Texas Red-conjugated donkey anti-mouse antibody. B5 was visualized by either GFP fluorescence (vB5R-GFP, vB5R-GFP/A33R<sup>C62S</sup>, or vB5R-GFP/ $\Delta$ A33R) or staining with an anti-B5 MAb, followed by FITC-conjugated donkey anti-rat antibody (WR, vA33R<sup>C62S</sup>, v $\Delta$ A33R). Cells were visualized using a fluorescent microscope. Localization of B5-GFP or B5 (green) and A33 (red) at the site of wrapping (concave arrowheads), at the cell vertices (arrows), and on virion-sized particles (arrowheads) are indicated. The DNA in nuclei and viral factories was stained with DAPI (blue). The overlap of green and red is shown as yellow.

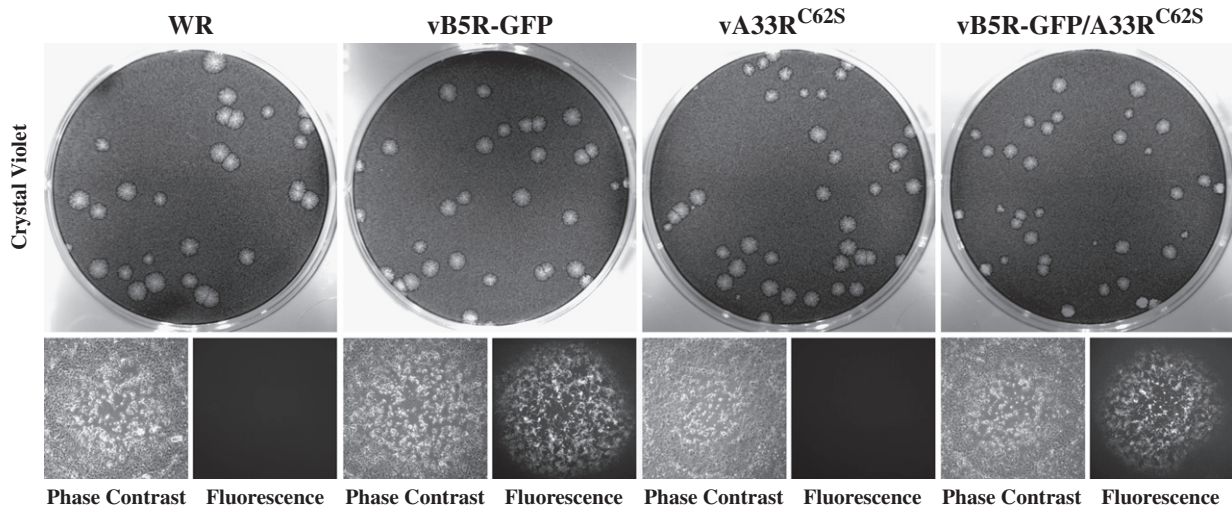


**Fig. 6.** Recombinant viruses expressing A33R<sup>C62S</sup> form plaques that are similar in size to those made by their parental viruses. Confluent BS-C-1 cell monolayers were infected with the indicated viruses. 24 h PI, the inoculum was removed and cell monolayers were overlaid with semi-solid media. 2 days PI, fluorescence and phase contrast images of plaques were captured using a fluorescent microscope. Cell monolayers were subsequently stained with crystal violet and imaged.

However, vA33R<sup>C62S</sup> produces similar amount of infectious enveloped virions as WR (Figs. 7 and 8), indicating that A33 tetramers appear not to have an important role during infection.

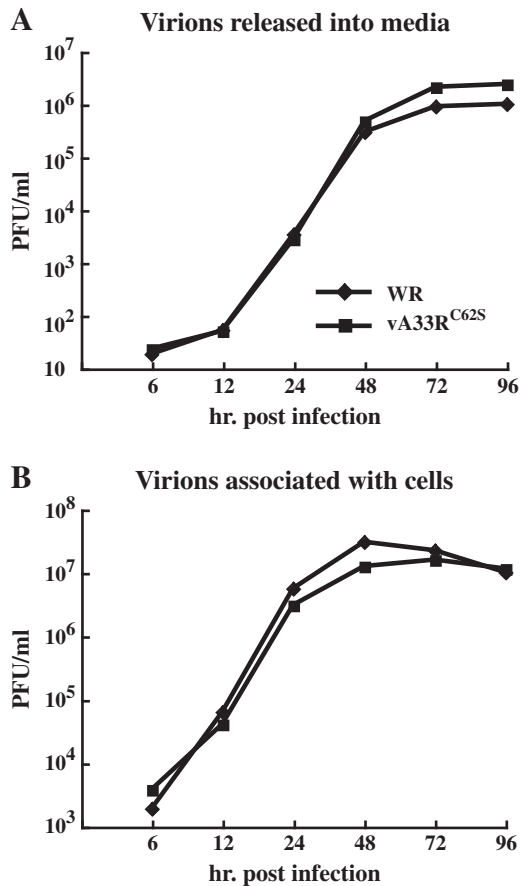


**Fig. 7.** vA33R<sup>C62S</sup> and WR produce similar amounts of infectious virions and spread at similar rates. BS-C-1 cells were infected with either WR or vA33R<sup>C62S</sup> at a MOI of 0.01 in duplicate. At the indicated times, supernatants were collected and cells were harvested by scraping in fresh media. Virions released into the media (A) or associated with the cells (B) were titered on fresh BS-C-1 cell monolayers. The averaged PFU/ml are shown.

Our data show that A33<sup>C62S</sup> still interacts with B5-GFP and forms homodimers (Figs. 2 and 3). It was interesting to find that A33-HA<sup>C100S</sup>, A33-HA<sup>C109S</sup>, A33-HA<sup>C126S</sup>, and A33-HA<sup>C180S</sup> co-immunoprecipitated a greater amount of B5 and B5-GFP than normal A33-HA<sup>C100S</sup> (Fig. 2). It is possible that disruption of intramolecular disulfide bond formation causes the protein structure to be in a more relaxed state and thus allows greater interaction with B5. In addition, A33-HA<sup>C100S</sup>, A33-HA<sup>C109S</sup>, A33-HA<sup>C126S</sup>, and A33-HA<sup>C180S</sup> migrated as a doublet on SDS-PAGE (Fig. 2). A33 has been shown to be glycosylated, and there are two putative N-linked glycosylation sites (Payne, 1992). However, it has not been shown if A33 is glycosylated at one or both sites. Mutating the cysteines at positions 100, 109, 128, or 180 may have exposed both of the glycosylation sites, and hence, the appearance of a slower migrating band in addition to the band consistent with normal A33-HA (Fig. 2). Mutants A33-HA<sup>C100S</sup>, A33-HA<sup>C109S</sup>, A33-HA<sup>C126S</sup>, and A33-HA<sup>C180S</sup> interacted stronger with V5-A33<sup>C62S</sup> than normal A33-HA, but not as well to themselves (Fig. 3), indicating that they appeared to dimerize better with V5-A33<sup>C62S</sup>. It is unclear why these mutants interact with A33<sup>C62S</sup> better than the normal A33.

## Materials and methods

### Construction of plasmids

Construction of pB5R-GFP has been described previously (Ward and Moss, 2000). To construct pA33R-HA, the coding sequence of A33R was amplified with a 5' primer and a 3' primer, which contains the coding sequence of influenza hemagglutinin (HA) epitope tag, using PCR. The resulting PCR fragment was inserted into pCR2.1 (Invitrogen) and subcloned into pcDNA3 (Invitrogen) that had been digested with *Hind*III and *Xho*I restriction enzymes. To mutate individual cysteines to serines, forward and reverse primers containing the desired mutation were generated. An overlapping two-step PCR was performed using pA33R-HA as the template. The resulting PCR fragments were inserted into pCR2.1 (Invitrogen) and subcloned into pcDNA3 (Invitrogen) as described above to generate pA33R-HA<sup>C36S</sup>, pA33R-HA<sup>C62S</sup>, pA33R-HA<sup>C100S</sup>, pA33R-HA<sup>C109S</sup>, and pA33R-HA<sup>C126S</sup>. To construct pA33R-HA<sup>C180S</sup>, PCR was performed using pA33R-HA as the template and a 5' primer and a 3' primer, which contains the desired mutation and the coding sequence of an HA epitope tag. To construct pA33R full, the coding sequence of A33R containing 500-bp upstream and downstream regions were amplified



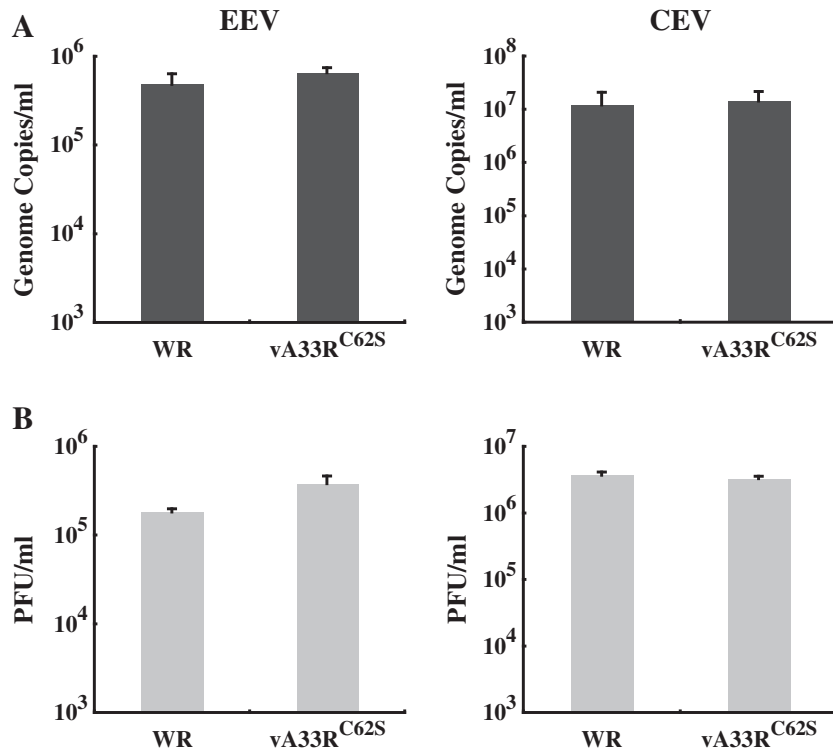


**Fig. 8.** vA33R<sup>C62S</sup> and WR produce similar amounts of EEV and CEV. BS-C-1 cells were infected with either WR or vA33R<sup>C62S</sup> at a MOI of 10.0 in duplicate. 24 h PI, EEV containing supernatants were collected and cell monolayers were incubated with media containing 1  $\mu$ g per ml of trypsin at 37 °C for 1 h. Afterward, the media was collected (CEV). The amounts of EEV and CEV produced were measured by absolute quantification of genome copies using real-time PCR (A) and their infectivity was determined by plaque assay on fresh BS-C-1 cell monolayers (B). The averages of EEV or CEV and the error bars for each virus are plotted.

using PCR. The PCR product was inserted into pCR2.1. pV5-A33R was constructed by digesting pV5-A33R fused to the coding sequence of YFP encoding 1 to 158 amino acids with *HindIII* and *BamHI*. The digested product was cloned to pCDNA3 (Invitrogen) that had been digested with *HindIII* and *BamHI*. To construct pA33R<sup>C62S</sup> full or pV5-A33R<sup>C62S</sup>, site-directed mutagenesis was performed using *pfu Turbo* DNA polymerase (Stratagene) and pA33R full or pV5-A33R, respectively, as the template. All constructs were verified by sequencing.

#### Construction of A33R<sup>C62S</sup> recombinants

Construction of vTF7.3, vB5R-GFP, WR, vB5R-GFP/ $\Delta$ A33R, and v $\Delta$ A33R has been described (Chan and Ward, 2010; Earl and Moss, 1991; Roper et al., 1998; Ward and Moss, 2001b). To generate vB5R-GFP/A33R<sup>C62S</sup> or vA33R<sup>C62S</sup>, cells infected with either vB5R-GFP/ $\Delta$ A33R or v $\Delta$ A33R, respectively, were transfected with pA33R<sup>C62S</sup> full. The next day, cells were harvested and cell lysates were plated on fresh BS-C-1 cells. Plaques were picked, purified, and amplified as described previously (Earl and Moss, 1991). The presence of the desired mutation in the recombinants was verified by sequencing.

#### Immunofluorescence microscopy

HeLa cells grown on coverslips were infected with vB5R-GFP, vB5R-GFP/A33R<sup>C62S</sup>, vB5R-GFP/ $\Delta$ A33R, WR, vA33R<sup>C62S</sup>, or v $\Delta$ A33R at a multiplicity of infection (MOI) of 1.0. The next day, fixed and permeabilized cells were stained with an anti-A33 MAb (10F10) (kindly provided by Jay Hooper), followed by Texas Red-conjugated donkey anti-mouse antibody (Jackson ImmunoResearch Laboratories). Cells infected with either WR, vA33R<sup>C62S</sup>, or v $\Delta$ A33R were stained with an anti-B5 MAb, followed by FITC-conjugated donkey anti-rat antibody (Jackson ImmunoResearch Laboratories). Coverslips were mounted as previously described (Chan and Ward, 2010). Cells were visualized and

imaged as previously described (Ward, 2005). Images were processed minimally and overlaid using Adobe Photoshop (Adobe).

#### Western blot analysis

HeLa cells were infected with vTF7.3 at a MOI of 5.0 and transfected with pA33R-HA or pA33R-HA cysteine-to-serine mutants in the presence of cytosine arabinoside (Sigma). The next day, cells were harvested and lysed in radioimmunoprecipitation assay (RIPA) buffer. Proteins were resolved on 4–12% Bis-Tris gels (Invitrogen) and transferred to nitrocellulose membranes. A33-HA or A33-HA cysteine-to-serine mutants were detected by Western blotting using a Horseradish peroxidase (HRP)-conjugated anti-HA antibody (Roche) or anti-A33 MAb (10F10), followed by an HRP-conjugated donkey anti-mouse antibody (Jackson ImmunoResearch Laboratories). To examine the expression of A33 during normal infection, HeLa cells were infected with WR, vA33R<sup>C62S</sup>, v $\Delta$ A33R, vB5R-GFP, vB5R-GFP/A33R<sup>C62S</sup>, or vB5R-GFP/ $\Delta$ A33R at a MOI of 5.0. The next day, cells were processed as described above. Western blot analysis was performed to detect A33 or A33<sup>C62S</sup> using an anti-A33 rabbit antiserum (BEI Resources), or anti-A33 MAb (10F10), followed by an HRP-conjugated donkey anti-rabbit or anti-mouse antibody, respectively (Jackson ImmunoResearch Laboratories). Bound antibodies were detected using chemiluminescent reagents (Pierce) according to manufacturer's instructions. B5-GFP was detected using an HRP-conjugated anti-GFP antibody.  $\beta$ -actin was detected using an anti- $\beta$ -actin MAb (Sigma), followed by an HRP-conjugated donkey anti-mouse antibody (Jackson ImmunoResearch Laboratories).

#### Co-immunoprecipitation

The procedure for immunoprecipitation has been described (Earley et al., 2008). Briefly, pA33R-HA or pA33R-HA cysteine-to-serine



mutants were co-transfected with either pB5R-GFP or pV5-A33R<sup>C62S</sup> into HeLa cells infected with vTF7.3 in the presence of AraC. The next day, cells were harvested and lysed as described above. To test the interaction with B5-GFP, transfection media was removed 4 h after later and replaced with media containing 50  $\mu$ Ci per milliliter of [<sup>35</sup>S]-Met/Cys. Cell lysates were subjected to immunoprecipitation with an anti-HA MAb (Santa Cruz Biotechnology). Antibody–protein complexes were pulled down using Protein G Agarose (CalBiochem), resolved on 4–12% Bis-Tris Gels (Invitrogen), and detected by autoradiography. To test dimerization of A33-HA cysteine-to-serine mutants, Western blot analysis was performed to detect V5-A33<sup>C62S</sup> using an HRP-conjugated anti-V5 antibody (Invitrogen).

#### Low MOI growth curves

The procedure for low MOI growth curves has been described previously (Ward, 2005). Briefly, BS-C-1 cells were infected with either WR or vA33R<sup>C62S</sup> at a MOI of 0.01 in duplicate. At 6, 12, 18, 24, 48, 72, and 96 h PI, EEV containing media were collected and cells were harvested by scraping in the media. Cells were frozen and thawed three times to release the virions associated with the cells. The amounts of infectious EEV and virions with the cells were determined by plaque assays on fresh BS-C-1 cell monolayers.

#### Quantification of EEV and CEV

The procedure for quantification of EEV and CEV has been described previously (Chan and Ward, 2010). Briefly, BS-C-1 cells were infected with WR or vA33R<sup>C62S</sup> at a MOI of 10.0. 24 h PI, EEV containing supernatants were collected. CEV were released by treatment of cell monolayers with trypsin. Amounts of EEV and CEV produced by the recombinants were determined by quantification of genome copies using real-time PCR. Infectious amounts of EEV and CEV produced were determined by plaque assays on BS-C-1 cells.

#### Acknowledgments

We thank Bernard Moss for the recombinant viruses and the plasmids and Jay Hooper for an anti-A33 MAb. Parts of this work were funded by National Institute of Allergy and Infectious Diseases grant AI067391 and contract N01-AI-50020. W.M.C. is supported by the National Institute of Allergy and Infectious Diseases Molecular Pathogenesis of Bacteria and Viruses Training grant T32 AI007362.

#### References

Appleyard, G., Hapel, A.J., Boulter, E.A., 1971. An antigenic difference between intracellular and extracellular rabbitpox virus. *J. Gen. Virol.* 13, 9–17.

Blasco, R., Moss, B., 1991. Extracellular vaccinia virus formation and cell-to-cell virus transmission are prevented by deletion of the gene encoding the 37,000-Dalton outer envelope protein. *J. Virol.* 65 (11), 5910–5920.

Buchman, G.W., Cohen, M.E., Xiao, Y., Richardson-Harman, N., Silvera, P., Detolla, L.J., Davis, H.L., Eisenberg, R.J., Cohen, G.H., Isaacs, S.N., 2010. A protein-based smallpox vaccine protects non-human primates from a lethal monkeypox virus challenge. *Vaccine* 28 (40), 6627–6636.

Chan, W.M., Ward, B.M., 2010. There is an A33-dependent mechanism for the incorporation of B5-GFP into vaccinia virus extracellular enveloped virions. *Virology* 402 (1), 83–93.

Chen, Z., Earl, P., Americo, J., Damon, I., Smith, S.K., Yu, F., Sebrell, A., Emerson, S., Cohen, G., Eisenberg, R.J., Gorshkova, I., Schuck, P., Satterfield, W., Moss, B., Purcell, R., 2007. Characterization of chimpanzee/human monoclonal antibodies to vaccinia virus A33 glycoprotein and its variola virus homolog in vitro and in a vaccinia virus mouse protection model. *J. Virol.* 81 (17), 8989–8995.

Duncan, S.A., Smith, G.L., 1992. Identification and characterization of an extracellular envelope glycoprotein affecting vaccinia virus egress. *J. Virol.* 66, 1610–1621.

Earl, P.L., Moss, B., 1991. Generation of recombinant vaccinia viruses. In: Ausubel, F.M., Brent, R., Kingston, R.E., Moore, D.D., Seidman, J.G., Smith, J.A., Struhl, K. (Eds.), *Current Protocols in Molecular Biology*, Vol. 2. Greene Publishing Associates & Wiley Interscience, New York. 16.17.1–16.17.16.

Earley, A.K., Chan, W.M., Ward, B.M., 2008. The vaccinia virus B5 protein requires A34 for efficient intracellular trafficking from the endoplasmic reticulum to the site of wrapping and incorporation into progeny virions. *J. Virol.* 82 (5), 2161–2169.

Engelstad, M., Howard, S.T., Smith, G.L., 1992. A constitutively expressed vaccinia gene encodes a 42-kDa glycoprotein related to complement control factors that forms part of the extracellular virus envelope. *Virology* 188, 801–810.

Fang, M., Cheng, H., Dai, Z., Bu, Z., Sigal, L.J., 2006. Immunization with a single extracellular enveloped virus protein produced in bacteria provides partial protection from a lethal orthopoxvirus infection in a natural host. *Virology* 345 (1), 231–243.

Fogg, C., Lustig, S., Whitbeck, J.C., Eisenberg, R.J., Cohen, G.H., Moss, B., 2004. Protective immunity to vaccinia virus induced by vaccination with multiple recombinant outer membrane proteins of intracellular and extracellular virions. *J. Virol.* 78 (19), 10230–10237.

Geada, M.M., Galindo, I., Lorenzo, M.M., Perdiguero, B., Blasco, R., 2001. Movements of vaccinia virus intracellular enveloped virions with GFP tagged to the F13L envelope protein. *J. Gen. Virol.* 82 (Pt 11), 2747–2760.

Golden, J.W., Hooper, J.W., 2008. Heterogeneity in the A33 protein impacts the cross-protective efficacy of a candidate smallpox DNA vaccine. *Virology* 377 (1), 19–29.

Grosenbach, D.W., Hansen, S.G., Hruby, D.E., 2000. Identification and analysis of vaccinia virus palmitoylproteins. *Virology* 275 (1), 193–206.

Hiller, G., Weber, K., 1985. Golgi-derived membranes that contain an acylated viral polypeptide are used for vaccinia virus envelopment. *J. Virol.* 55 (3), 651–659.

Hollinshead, M., Rodger, G., Van Eijl, H., Law, M., Hollinshead, R., Vaux, D.J., Smith, G.L., 2001. Vaccinia virus utilizes microtubules for movement to the cell surface. *J. Cell Biol.* 154 (2), 389–402.

Hooper, J.W., Custer, D.M., Schmaljohn, C.S., Schmaljohn, A.L., 2000. DNA vaccination with vaccinia virus L1R and A33R genes protects mice against a lethal poxvirus challenge. *Virology* 266 (2), 329–339.

Hooper, J.W., Custer, D.M., Thompson, E., 2003. Four-gene-combination DNA vaccine protects mice against a lethal vaccinia virus challenge and elicits appropriate antibody responses in nonhuman primates. *Virology* 306 (1), 181–195.

Hooper, J.W., Thompson, E., Wilhelmson, C., Zimmerman, M., Ichou, M.A., Steffen, S.E., Schmaljohn, C.S., Schmaljohn, A.L., Jahrling, P.B., 2004. Smallpox DNA vaccine protects nonhuman primates against lethal monkeypox. *J. Virol.* 78 (9), 4433–4443.

Isaacs, S.N., Wolfe, E.J., Payne, L.G., Moss, B., 1992. Characterization of a vaccinia virus-encoded 42-kilodalton class I membrane glycoprotein component of the extracellular virus envelope. *J. Virol.* 66 (12), 7217–7224.

Lawrence, S.J., Lottenbach, K.R., Newman, F.K., Buller, R.M., Bellone, C.J., Chen, J.J., Cohen, G.H., Eisenberg, R.J., Belshe, R.B., Stanley Jr., S.L., Frey, S.E., 2007. Antibody responses to vaccinia membrane proteins after smallpox vaccination. *J. Infect. Dis.* 196 (2), 220–229.

McIntosh, A.A., Smith, G.L., 1996. Vaccinia virus glycoprotein A34R is required for infectivity of extracellular enveloped virus. *J. Virol.* 70 (1), 272–281.

Moss, B. (2001). *Poxviridae: The viruses and their replication*. Fourth ed. In "Fields Virology" (B. N. Fields, D. M. Knipe, and P. M. Howley, Eds.), Vol. 2, pp. 2849–2883. 2 vols. Lippincott-Raven Publishers, Philadelphia.

Payne, L.G., 1980. Significance of extracellular enveloped virus in the in vitro and in vivo dissemination of vaccinia. *J. Gen. Virol.* 50 (1), 89–100.

Payne, L.G., 1992. Characterization of vaccinia virus glycoproteins by monoclonal antibody preparations. *Virology* 187, 251–260.

Perdiguero, B., Blasco, R., 2006. Interaction between vaccinia virus extracellular virus envelope A33 and B5 glycoproteins. *J. Virol.* 80 (17), 8763–8777.

Rietdorf, J., Ploubidou, A., Reckmann, I., Holmstrom, A., Frischknecht, F., Zettl, M., Zimmermann, T., Way, M., 2001. Kinesin-dependent movement on microtubules precedes actin-based motility of vaccinia virus. *Nat. Cell Biol.* 3 (11), 992–1000.

Roper, R.L., Payne, L.G., Moss, B., 1996. Extracellular vaccinia virus envelope glycoprotein encoded by the A33R gene. *J. Virol.* 70 (6), 3753–3762.

Roper, R.L., Wolfe, E.J., Weisberg, A., Moss, B., 1998. The envelope protein encoded by the A33R gene is required for formation of actin-containing microvilli and efficient cell-to-cell spread of vaccinia virus. *J. Virol.* 72 (5), 4192–4204.

Schmelz, M., Sodeik, B., Ericsson, M., Wolfe, E.J., Shida, H., Hiller, G., Griffiths, G., 1994. Assembly of vaccinia virus: the second wrapping cisterna is derived from the trans Golgi network. *J. Virol.* 68 (1), 130–147.

Smith, G.L., Vanderplassen, A., Law, M., 2002. The formation and function of extracellular enveloped vaccinia virus. *J. Gen. Virol.* 83 (Pt 12), 2915–2931.

Su, H.P., Singh, K., Gittis, A.G., Garboczi, D.N., 2010. The structure of the poxvirus A33 protein reveals a dimer of unique C-type lectin-like domains. *J. Virol.* 84 (5), 2502–2510.

Tooze, J., Hollinshead, M., Reis, B., Radsak, K., Kern, H., 1993. Progeny vaccinia and human cytomegalovirus particles utilize early endosomal cisternae for their envelopes. *Eur. J. Cell Biol.* 60 (1), 163–178.

van Eijl, H., Hollinshead, M., Smith, G.L., 2000. The vaccinia virus A36R protein is a type Ib membrane protein present on intracellular but not extracellular enveloped virus particles. *Virology* 271 (1), 26–36.

van Eijl, H., Hollinshead, M., Rodger, G., Zhang, W.H., Smith, G.L., 2002. The vaccinia virus F12L protein is associated with intracellular enveloped virus particles and is required for their egress to the cell surface. *J. Gen. Virol.* 83 (Pt 1), 195–207.

Wagenaar, T.R., Moss, B., 2007. Association of vaccinia virus fusion regulatory proteins with the multicomponent entry/fusion complex. *J. Virol.* 81 (12), 6286–6293.

Ward, B.M., 2005. Visualization and characterization of the intracellular movement of vaccinia virus intracellular mature virions. *J. Virol.* 79, 4755–4763.

Ward, B.M., Moss, B., 2000. Golgi network targeting and plasma membrane internalization signals in vaccinia virus B5R envelope protein. *J. Virol.* 74 (8), 3771–3780.

- Ward, B.M., Moss, B., 2001a. Vaccinia virus intracellular movement is associated with microtubules and independent of actin tails. *J. Virol.* 75 (23), 11651–11663.
- Ward, B.M., Moss, B., 2001b. Visualization of intracellular movement of vaccinia virus virions containing a green fluorescent protein-B5R membrane protein chimera. *J. Virol.* 75 (10), 4802–4813.
- Ward, B.M., Weisberg, A.S., Moss, B., 2003. Mapping and functional analysis of interaction sites within the cytoplasmic domains of the vaccinia virus A33R and A36R envelope proteins. *J. Virol.* 77 (7), 4113–4126.
- Wolfe, E.J., Weisberg, A.S., Moss, B., 2001. The vaccinia virus A33R protein provides a chaperone function for viral membrane localization and tyrosine phosphorylation of the A36R protein. *J. Virol.* 75 (1), 303–310.